



**HAL**  
open science

# High temperature oxidation behavior of chromium-rich alloys containing high carbides fractions. Part I: Nickel-base alloys

Patrice Berthod

► **To cite this version:**

Patrice Berthod. High temperature oxidation behavior of chromium-rich alloys containing high carbides fractions. Part I: Nickel-base alloys. *Materials and Corrosion / Werkstoffe und Korrosion*, 2013, 64 (7), pp.567-577. 10.1002/maco.201106250 . hal-02541177

**HAL Id: hal-02541177**

**<https://hal.science/hal-02541177>**

Submitted on 13 Apr 2020

**HAL** is a multi-disciplinary open access archive for the deposit and dissemination of scientific research documents, whether they are published or not. The documents may come from teaching and research institutions in France or abroad, or from public or private research centers.

L'archive ouverte pluridisciplinaire **HAL**, est destinée au dépôt et à la diffusion de documents scientifiques de niveau recherche, publiés ou non, émanant des établissements d'enseignement et de recherche français ou étrangers, des laboratoires publics ou privés.

# **High temperature oxidation behaviour of chromium-rich alloys containing high carbides fractions. Part I: Nickel-base alloys**

Patrice Berthod\*

Institut Jean Lamour (UMR CNRS 7198), department Chemistry and Physic of Solids and Surfaces

Faculty of Science and Technologies, B.P. 70239, 54506 Vandoeuvre-lès-Nancy, France

E-mail: pberthodcentralelille1987@orange.fr

Tel. (+33) 3 83 68 46 66

Fax (+33) 3 83 68 46 11

*Postprint version of the article **Materials and Corrosion** 2013, 64, No. 7 pp. 567-577*

DOI: 10.1002/maco.201106250

## **Summary:**

Six wear-resistant alloys based on nickel, containing 30wt.% Cr and from 2.5 to 5.0wt.%C, were elaborated by foundry and subjected to oxidation by air at 1000, 1100 and 1200°C, for evaluating the oxidation behaviour of hard bulk alloys. Their microstructures are rich in chromium carbides, eutectic or pro-eutectic, and they also contain graphite for the highest carbon contents of interest. All the studied alloys obviously display a chromia-forming behaviour, despite the initial low chromium content in the matrix. During oxidation carbides disappear over an increasing distance from the oxidation front, with as consequence the enrichment of the neighbor matrix in chromium. The minimal chromium content on surface after oxidation decreases when the alloy is richer in carbon and increases with the oxidation temperature. The carbide-free zone tends to be deeper when the oxidation temperature increases, and also when the alloy's carbon content increases, in contrast with low-C Ni-30Cr alloys previously studied. The disappearance of carbides means a carbon loss as gaseous oxidized species. This probably disturbs the oxide scales growing on the external surface and may influence the oxidation behaviour of the alloys. When present, graphite does not deteriorate dramatically the oxidation resistance of the alloys. The hardness of the alloys are lowered by the exposures to high temperature and by the presence of graphite.

## **Keywords:**

Nickel alloys; High carbon contents; Chromium carbides; Graphite; High temperature Oxidation

## 1 Introduction

The cast nickel-base alloys rich in chromium are employed in various fields, from low temperature (e.g. frameworks reinforcing dental prostheses [1-3]) to temperatures much higher (e.g. the hottest parts of aero-engines [4-6]). Whatever the considered application chromium plays a very important role in the corrosion resistance of the alloys, by aqueous solutions as well as by hot oxidant gases. Chromium is also an important carbide-former element, stronger than nickel, and in presence of carbon it can lead to chromium carbides which can be of different types ( $\text{Cr}_{23}\text{C}_6$ ,  $\text{Cr}_7\text{C}_3$ ,  $\text{Cr}_3\text{C}_2$ , ...), with consequently important modifications of some mechanical properties of the alloys: tensile strength and creep-resistance at high temperature for moderate carbides fractions, high levels of hardness for high carbide fractions. In the latter case an interesting set of properties can result from the association of a ductile FCC nickel-based matrix and of numerous dispersed hard chromium carbides, e.g. not too low ductility with high hardness, as required for wear resistance [7-9].

In service the wear-solicited materials or coatings may reach high temperatures and they can be affected by oxidation by hot air. Several studies have been already carried out on the oxidation behaviour at around  $1000^\circ\text{C}$  of  $\text{Cr}_3\text{C}_2$ -rich nickel-based coatings deposited by various techniques: detonation spray [10], thermal spray [11] or high velocity oxy fuel (HVOF) spray [12]. However it appears that hard alloys containing high fractions of carbides elaborated by foundry as bulk materials, as well as their behaviour in high temperature oxidation, were not so extensively studied. The aim of the present work is to elaborate by conventional casting a set of six nickel alloys containing the same high chromium content, and carbon with a content increasing from 2.5 to 5wt.%C, and thereafter to subject them to air at three high temperatures to examine how they can be deteriorated by oxidation.

## 2 Experimental details

Six compositions  $\{\text{Ni-30wt.\%Cr}\}+\text{C}$  with a weight carbon content equal to 2.5 (alloy "Ni25"), 3.0 ("Ni30"), 3.5 ("Ni35"), 4.0 ("Ni40"), 4.5 ("Ni45") and 5.0wt.% ("Ni50") were considered in this study. Thermodynamic calculations were first performed using the Thermo-Calc software [13] working with a database containing the descriptions of the Ni-Cr-C system and of its sub-systems [14 - 16]. This was done to anticipate the stable microstructures that will be shown by the corresponding real alloys at the temperatures of the oxidation tests, and also the chromium repartition between matrix and the chromium carbides. Thermo-Calc was thereafter also used to obtain some information about carbon in the sub-surface after oxidation.

The six alloys were elaborated by foundry under an atmosphere of 300mbar of argon gas, from pure elements (>99.9%, Alfa Aesar) using a high frequency induction furnace (CELES). Fusion and solidification were achieved in the water-cooled copper crucible of the furnace. The masses of the obtained ingots were about 40g. In these ingots compact samples of about  $125\text{ mm}^3$  were cut to obtain several samples. Per ingot one sample was prepared for the examination of the as-cast microstructure, and the three others were destined to the oxidation tests.

After surface preparation, one sample per alloy was exposed to the laboratory air at 1000°C for 50 hours in a resistive tubular furnace before cooling outside in ambient air. The second one was exposed at 1100°C and the third one at 1200°C, with the same other conditions.

The as-cast samples and the oxidized samples were embedded in a cold resin mixture (Araldite CY230 + Strengthener Escil HY956). The embedded samples were thereafter cut in two parts using a Buehler Isomet 5000 precision saw, then polished with SiC papers under water (from 120 to 1200 grit), and finished with textile paper enriched with 1µm–alumina particles. A Scanning Electron Microscope (SEM, XL30 Philips) was used for the metallographic observations, performed essentially in the Back Scattered Electrons mode (BSE) and under an acceleration voltage of 20 kV. The bulk of the oxidized samples were additionally characterized by X-Ray Diffraction using a Philips X-Pert Pro diffractometer (wavelength Cu K $\alpha$ ) to better know the nature of the carbides at the temperatures of the oxidation tests (carbides assumed to have not changed during the fast cooling down to ambient temperature by air quenching). WDS profiles (Wavelength Dispersion Spectrometry) were performed using a Cameca SX100 microprobe, across the oxide scales still present on surface and the alloys' sub-surfaces affected by oxidation, in order to better know the oxides' natures and the chromium depletion.

The possible hardness evolution in the bulk during the oxidation tests were also investigated by applying Vickers indentations with a load of 30kg, using a Testwell Wolpert apparatus.

### 3 Results of the thermodynamic calculations

According to thermodynamic calculations all the alloys ought to be of a hyper-eutectic type since their solidification would start by the crystallization of carbides ( $M_7C_3$  for Ni25, Ni30 and Ni35,  $M_3C_2$  for Ni40) or of graphite (Ni45 and Ni50). This is confirmed by the observations done on the as-cast microstructures illustrated by some SEM/BSE micrographs in Figure 1, in which one can see the more (Ni25-Ni30) or less (Ni35-Ni50) elongated carbides forming a eutectic with the matrix, the coarse acicular pro-eutectic carbides (more present in the carbon-richest alloys), and the lamellar graphite in Ni45 and Ni50. Graphite is also present in Ni40 (Fig. 2(a)) but these particles are rarer and more compact than in Ni45 and Ni50 (Fig. 2(b)).

The microstructures of the alloys at the three temperatures of oxidation tests are described in Table 1 (natures of the phases present) and Table 2 (mass fractions of matrix and chromium contents in matrix). The two first alloys (Ni25 and Ni30) ought to contain FCC nickel-based matrix forming a eutectic with carbides, pro-eutectic and eutectic carbides of two types ( $M_7C_3$  and  $M_3C_2$ ) at 1000 and 1100°C. At 1200°C the carbides present are a mix of  $M_7C_3$  and  $M_3C_2$  for 3wt.% but there are only  $M_7C_3$  for 2.5wt.%C. The Ni35 alloy qualitatively keeps the same microstructure at the three temperatures (FCC matrix + pro-eutectic and eutectic  $M_3C_2$ ), and the three carbon-richest alloys contain a eutectic matrix, eutectic and pro-eutectic  $M_3C_2$  carbides, and also graphite.

In all cases the matrix is the main phase present (always more than 70% of the alloy in mass) but its mass fraction depends on the carbon content. For example, at 1000°C, it decreases from 76% to 72% when the carbon content increases from 2.5 (Ni25 alloy) to 5wt.% (Ni50). The mass fraction of matrix tends to increase when the stage temperature increases, except when there is a progressive change from  $M_3C_2$  to  $M_7C_3$  (Ni25 and Ni30).

Despite the presence of nickel accompanying chromium in the carbides (e.g. Ni is between 10 and 20% of the M element in  $M_7C_3$  at the eutectic temperature, according to Thermo-Calc), the  $M_7C_3$  and  $M_3C_2$  carbides are very rich in chromium (between 70 and 80% of Cr in  $M_7C_3$  and about 86% of Cr in  $M_3C_2$ , at the eutectic temperature,

according to Thermo-Calc). Thus, their presence in great quantities (between 24 and 28% of the mass of the alloy) induces a severe impoverishment in chromium for the matrix, by comparison to similar nickel alloys with much lower carbon contents (for which the main part of the 30wt.% of chromium is present in matrix). For the alloys of interest in the present study the chromium contents in the matrix are very low, from almost 14wt.% in the Ni25 matrix at 1200°C to only almost 9wt.% in the Ni40, Ni45 and Ni50 alloys at 1000°C. One can note, for the three later alloys, that the increase in carbon from Ni40 to Ni50 profits only to graphite.

#### **4 Metallography results after the high temperature oxidation tests**

The surface states of all the alloys after oxidation at the three temperatures are illustrated by SEM/BSE micrographs in Figure 3 for the Ni25, Ni30 and Ni35 alloys, and in Figure 4 for the Ni40, Ni45 and Ni50 alloys. All the samples were covered by external oxide scales but these ones were damaged during the isothermal stage (internal growth stresses in oxides, gas formation by carbon oxidation between external scale and the substrate) and partly lost during the post-test cooling since only some parts of oxides were still present on the alloys at room temperature, as seen in the cross sections metallographically examined. The oxide scales were composed of chromia, as shown by the concentration profiles given as examples in Figure 5, other oxides being additionally present in some cases. Internal oxidation obviously also occurred, as shown by the presence of internal oxides and by some coarse carbides being oxidized (e.g. micrograph of Ni50 at 1100°C in Figure 3). In all cases carbides disappeared from the surface (oxide/alloy interface), over a depth which increases with the temperature of oxidation test. The values of the average depth of this carbide-free zone measured on three different micrographs for an alloy and one temperature (with the calculated standard deviation for uncertainty), are given in Table 3. There is effectively an increase of this carbide-free depth with temperature for all alloys, but no clear evolution versus the carbon content (even if there is a tendency for an increase of this depth with the carbon content). In some cases more or less thick and elongated oxide areas exist in the carbide-free zone, as illustrated for one oxidized sample by the micrograph presented in Figure 6 and detected in other cases by WDS concentrations profiles revealing more or less thick Cr<sub>2</sub>O<sub>3</sub> inclusions.

Concentrations profiles were obtained for all the oxidized samples by WDS measurements performed perpendicularly to the external surface across the oxide scale and the sub-surface affected by oxidation. These profiles generally show a chromium depletion, but this phenomenon usually met in chromia-forming refractory alloys is here often difficult to evidence because of the rather thin carbide-free zones and the high density of carbides present deeper. Nevertheless it was possible to extract first the minimal chromium content near the surface for all oxidized alloys, and to estimate the average chromium concentration gradients for the alloys oxidized at 1200°C. The values are given in Table 4. It appears first that the average level of chromium content in the carbide-free zones, and even a little deeper, are significantly higher than the theoretic contents in matrix previously estimated by the thermodynamic calculations. Second, the minimal chromium contents near the surfaces after oxidation at 1200°C tend to decrease when the alloy's carbon content increases; this decrease in chromium also exists after oxidation at 1000 and 1100°C from 2.5 to 4wt.%C in the alloy while it seems almost constant between 4 and 5wt.%C. In addition this minimal chromium content tends to increase when the temperature of oxidation test increases, notably between 1100 and 1200°C.

## 5 Balance sheets in chromium and in carbon for the sub-surfaces

By calculating for each alloy the difference between the average chromium content in the carbide-free zone and 30wt.% (initial content), and assuming that there was no backward movement of the {external oxide / alloy} interface during the oxidation tests (because alloy consumption), it is possible to estimate the quantity of chromium having leaved the alloy to form the chromia external scale and, for the two highest temperatures, the volatile oxide  $\text{CrO}_3$ . The values are given in Table 5 in which the intervals result from the {average  $\pm$  standard deviation} interval of carbide-free zone depth. In general the mass of chromium lost by the alloys during the 50 hours of oxidation tends increasing from Ni25 to Ni50, and also increasing with temperature. However there are particular results for Ni25, consequence of its deep carbide-free zones at the three temperatures.

The main part of the carbon atoms released by the disappearing carbides have obviously lost the alloys since they cannot exist in the carbide-free zone. Indeed, as previously used in other studies [17, 18] thermodynamic calculations allowed here specifying the maximal carbon contents authorized by the absence of carbides for the average chromium content in the carbide-free zone. The isothermal sections of the Ni-Cr-C diagram computed with Thermo-Calc for 1000, 1100 and 1200°C presented in Figure 7 effectively show that the carbon contents in the carbide-free zones must be lower than few tens weight percents, which is negligible by comparison with the 2.5 to 5wt.% of carbon initially present. Thus, by neglecting the carbon contents in the carbide-free zones one can assess the masses of carbon having leaved the alloys as gaseous oxidized species. The obtained values are also given in Table 6 and they follow, except for Ni25, the same trend as chromium: increase when the alloy is richer in carbon and also increase when the temperature of oxidation is higher.

## 6 Microstructure and hardness evolutions in the bulk

The exposures to high temperature during the oxidation test were long enough to induce consequences for the microstructures in the bulk of the alloys. In fact, compared to the as-cast microstructures the shapes and fractions of the carbides are not significantly changed, except for the samples oxidized at the highest temperature since their carbides are obviously rounder and their total surface fractions are slightly decreased. This can be seen by comparing the bottom parts of the micrographs presented in Figure 3 and Figure 4 to the microstructures illustrated in Figure 1. In contrast their types (issued from solidification) may have changed to correspond to the thermodynamic equilibria at the stage temperatures. The X-Ray Diffraction spectra (two examples are displayed in Figure 8 and Figure 9) indicate that carbides are now conform to the types predicted by Thermo-Calc (Table 1). The stage durations at high temperature were long enough to allow the eventual transformation of the carbides to the most thermodynamically stable types, and the cooling in air was fast enough to do not allow a new transformation of these carbides.

Vickers indentations were performed for all the alloys in the as-cast condition and in their three aged states. One can see that, in all cases, the hardness increases with the carbon content from 2.5 to 3.5wt.% then decreases from 3.5 to 5wt.%C (Figure 10). For a given carbon content in alloy, hardness is higher for the as-cast condition than for the three aged states. Further, the hardness of an alloy exposed to 1100°C is almost the same as its hardness after exposure to 1000°C, while an exposure at 1200°C leads to significantly lowered hardness for all the alloys.

## 7 Discussion

Such bulk alloys elaborated by classical casting, instead by thermal spray or other coating deposition techniques, led to rather coarse microstructures, with a lot of carbides rich in chromium ( $\text{Cr}_3\text{C}_2$ , and notably  $\text{Cr}_7\text{C}_3$ ) among which feature particularly coarse pro-eutectic carbides. Consequently the initial matrix is necessarily dramatically impoverished in chromium (less than 15wt.% for all alloys and even less than 10wt.% for the carbon-richest ones). This let think to a very deteriorated oxidation behaviour of the whole alloys because of a continuous phase poor in chromium. Indeed, in absence of aluminium, a minimum of 20wt.%Cr is generally required for nickel base alloys to be chromia-former [19, 20]). One can initially think that the alloy maybe not helped by carbides the dissolution of which can be too slow (especially for the coarse pro-eutectic carbides) for allowing the supply of chromium enough to constitute and to maintain an external continuous chromia layer protecting the alloys [21]. Further, the presence of graphite may lead to sites of possible intense gassing by oxidation of free carbon.

In fact, the development of a carbide-free zone in all alloys after the oxidation shows that carbides are able to dissolve with a sufficient rate to release their chromium atoms which enter the neighbor matrix. This allows the matrix recovering a chromium content high enough, not only on extreme surface but in average in the whole carbide-free zone and the neighbor bulk part where carbides are dissolving, as shown by the microprobe results. This allowed obtaining protective chromia on surface during oxidation. But the dissolution of such high quantities of carbides also induces the release of high quantities of carbon (Table 6) which necessarily diffused towards the oxidation front where they are oxidized into gases. The resulting total gas volume for the oxidation duration (50h), estimated from the carbon masses given in Table 6 by using the molar gas volume and the perfect gas state law to extrapolate at high temperature, varies from about 2mL / cm<sup>2</sup> (for Ni25 at 1000°C) to about 55mL/cm<sup>2</sup> (for Ni45 at 1200°C). Since the kinetic of development of the carbide-free zone is almost parabolic (as previously observed for lower-carbon 30wt.%Cr-containing nickel-base alloys for the same temperatures and atmospheres) the greatest part of this CO<sub>x</sub> volume is liberated during the first hours of oxidation. This essentially perturbed the first stages of external oxide formation, but the forming gas volume was also of importance for the growing conditions and adherence of the external oxide scale until the end of the oxidation tests. This can partly explain that the observed external oxide is much less continuous as observed on Ni-30Cr-xC (with x<1wt.%) alloys [22]. In addition, oxide spallation phenomena may have also occurred during cooling.

If carbides – fine eutectic or coarse pro-eutectic – generally disappear and release their carbon and chromium atoms in the neighbor matrix instead being oxidized, it was sometimes found in the cross-sections of the mounted oxidized samples that the coarse carbides oriented almost perpendicularly to the extreme surface can be directly oxidized (example in the micrograph of Ni50 oxidized at 1100°C presented in Figure 4), as also encountered in  $\text{Cr}_3\text{C}_2$ -NiCr composites coatings [23]. This may locally change the oxidation progress. When such coarse elongated carbides close to the oxidation front are on the contrary almost parallel to the extreme surface it seems that they may be in some cases partly oxidized – by internal oxidation - before being totally dissolved, resulting in the persistence of a thick internal chromia film (Figure 6). Such internal oxide may favor a detachment of a part of alloy during the high temperature stage (with consequently oxidation all around the detached alloy part as seen in the micrographs of Ni25 and Ni35 both oxidized at 1200°C in Figure 3), or during the cooling (Figures 3 and 4, Ni35 oxidized at 1100°C and Ni50 oxidized at 1000°C) under the thermal and/or

mechanical stresses developed between the external part (carbide-free) and the internal part (still carbide-containing) of the alloy sample. Concerning the graphite initially present in the carbon-richest alloys one observed that this phase totally disappeared in the sub-surface affected by oxidation, consequently to the impoverishment in carbon due to the outward diffusion of this element, without other consequences for the oxidation phenomena.

It can be interesting to compare the oxidized states of these carbon-rich alloys to the ones of other ternary 30wt.%Cr-containing nickel alloys also exposed to 1000, 1100 and 1200°C during 50 hours in previous studies. Figure 11 presents for the three temperatures the evolution, versus the alloy's carbon content, of the minimal chromium content on surface (a), of the average carbide-free depth (b) and of the average chromium gradient in carbide-free zone (c and d) (only 1200°C for the alloys of the present study), from 0 to 5wt.%, by adding to the present results the ones previously obtained for the [0; 0.8wt.%C] and [1.2; 2.0wt.%C] intervals of alloy's carbon content (references: respectively [22] and [24]). Despite the presence of an external chromia scale on their surfaces it appears that the present alloys are more threatened by the loss of their chromia-forming behaviour and then by a catastrophic oxidation, than the alloys with less than 2.5wt.%C, because of their chromium contents on extreme surface which are significantly lower. Second, in contrast with the alloys containing from 0.2 to 2.0wt.%C for which the depth of the carbide-free zone regularly decreased when the carbon content increased, there is rather an increase of this depth with the carbon content. The latter observation is especially true for the two highest oxidation temperatures, for which the carbide-free zones are also particularly deep (notably for 1200°C) which let think to an oxidation particularly fast. For the same alloys, the average chromium gradient (after oxidation at 1200°C) tends to increase with the carbon content, also revealing a faster diffusion of chromium towards the oxidation front. The chromium having diffused and leaved the alloy during oxidation is then in greater quantities both for higher temperatures and for higher carbon contents (Table 5), showing in the second case that richer in carbon the alloy is, faster its oxidation is. However, even for the carbon-richest alloys and for 1200°C, catastrophic oxidation was not started after 50 hours but it appears imminent by considering the low chromium contents on extreme surface.

Concerning hardness, its bell-shape curve of evolution versus the carbon content in the alloy (due to the fraction increase in hard carbides (more than 1000Hv [25, 26] - and to the appearance of graphite - is shifted down by the 50 hours stages at 1000 and 1100°C, and a second time, by the stage at 1200°C. This softening of the alloys is a consequence of the less (1000 and 1100°C, not really visible on micrographs) or more (1200°C, easily evidenced) pronounced changes of shape and volume fraction of the carbides induced by the long times spent at high temperatures. Thus, such long exposures to high temperature led to a loss of hardness, and probably of wear-resistance, severe for the surface/sub-surface (carbide-free zones), and more limited for the bulk (carbide evolution due to interfacial energy minimization).

## 8 Conclusion

Although a global chromium content generally considered, for nickel-base refractory alloys and superalloys ,as high enough to ensure a chromia-forming behavior, several characteristics of the studied alloys elaborated by foundry as bulk materials can be initially considered as detrimental for their resistance against oxidation at high temperature: rather low chromium content in the metallic matrix, great part of chromium trapped by the

numerous carbides (among them some are very coarse) and then difficult to dissolve for releasing chromium, in some cases presence of graphite potentially easy to rapidly oxidize, high carbon quantities in whole alloy possibly leading to great volumes of gases after oxidation with consequently perturbation of the eventual protective oxide scale, ... Nevertheless the high temperature oxidation behaviours of these alloys were never catastrophic, even after a long duration at so high temperatures. In contrast, the development of a carbide-free zone induces the replacement of the initial hard surface by a much softer one, which can be a problem for the wear resistance. Fortunately the parts of surface which may be exposed to friction in service are not the same as the ones which can be exposed to oxidation because of the heating of the preceding neighbor zones.

#### **Acknowledgments:**

The author wishes thank E.Souaillat, O. Hestin, M. Ba and A. Dia for their contributions to this work, P. Villeger and Th. Schweitzer for their technical help, and also the Common Service of Microanalysis of the Faculty of Science and Technologies of Nancy.

#### **References:**

- [1] A. C. Quaas, S. Heide, S. Freitag, M. Kern, *Dental Materials*, 2005, 21(3), 192.
- [2] M. Dundar, M. A. Gungor, E. Cal, A. Darcan, A. Erdem, *General Dentistry*, **2007**, 55(3), 204.
- [3] R. Tiozzi, H. Falcão-Filho, F. A. Aguiar Junior, R. C. Rodrigues, M. D. G. Mattos, R. F. Ribeiro, *Journal of Oral Rehabilitation*, **2010**, 37(5), 359.
- [4] N. V. Russel, F. Wigley, J. Williamson, *Journal of Materials Science*, **2000**, 35, 2131.
- [5] G. Lvov, V. I. Levit, M. J. Kaufman, *Metallurgical and Materials Transactions A: Physical Metallurgy and Materials Science*, **2004**, 35A(6), 1669.
- [6] E. Lvova, *Journal of Materials Engineering and Performance*, **2007**, 16(2), 254.
- [7] E. Blank, E. Luchsinger, *Wear*, **1987**, 117(3), 289.
- [8] R. L. Sun, Y. W. Lei, W. Niu, *Surface and Coatings Technology*, **2009**, 203(10-11), 1395.
- [9] G. Fu, S. Liu, J. Fan, *Nuclear Engineering and Design*, **2011**, 241, 1403.
- [10] J. Wang, L. Zhang, B. Sun, Y. Zhou, *Surface and Coating Technology*, **2000**, 130(1), 69.
- [11] C. T. Kunioshi, O. V. Correa, L. V. Ramanathan, *Materials Research*, **2005**, 8(2), 125.
- [12] C. T. Kunioshi, O. V. Correa, L. V. Ramanathan, *Surface Engineering*, **2006**, 22(2), 121.
- [13] Thermo-Calc version N: "Foundation for Computational Thermodynamics" Stockholm, Sweden, Copyright (1993, 2000). [www.thermocalc.com](http://www.thermocalc.com)
- [14] A. Dinsdale, T. Chart: MTDS NPL, unpublished work, **1986**.
- [15] A. Gabriel, C. Chatillon, I. Ansara, *High Temperature Science*, **1988**, 25, 17.
- [16] J. O. Andersson, *Calphad*, **1987**, 11, 271.
- [17] P. Berthod, S. Michon, J. Di Martino, S. Mathieu, S. Noël, R. Podor, C. Rapin, *Calphad*, **2003**, 27, 279.
- [18] P. Berthod, C. Vébert, L. Aranda, R. Podor, C. Rapin, *Oxidation of Metals*, **2005**, 63(1/2), 57.
- [19] C. T. Sims, W. C. Hagel, *The Superalloys*, John Wiley & Sons, 1972.
- [20] E. F. Bradley, *Superalloys: A technical guide*, ASM International, 1988.
- [21] P. Kofstad, *High Temperature Corrosion*, Elsevier applied science, 1988.
- [22] P. Berthod, *Annales de Chimie – Science des Matériaux*, **2008**, 33(3), 247.

- [23] S. Matthews, B. James, M. Hyland, *Corrosion Science*, **2009**, 51, 1172.
- [24] P. Berthod, P. Lemoine, L. Aranda, *Materials Science Forum*, **2008**, 595-598, 871.
- [25] P.T.B. Shaffer: Handbooks of High-Temperature materials N°1. Materials Index, Plenum Press, 1964.
- [26] G.V. Samsonov: Handbooks of High-Temperature materials N°2. Properties Index, Plenum Press, 1964.

## TABLES

Table 1. Phases present in the microstructures of the studied alloys at the temperatures of the oxidation tests (according to Thermo-Calc)

Phases	1000°C	1100°C	1200°C
Ni25	mat.FCC + M <sub>7</sub> C <sub>3</sub> + M <sub>3</sub> C <sub>2</sub>	mat.FCC + M <sub>7</sub> C <sub>3</sub> + M <sub>3</sub> C <sub>2</sub>	mat.FCC + M <sub>7</sub> C <sub>3</sub>
Ni30	mat.FCC + M <sub>7</sub> C <sub>3</sub> + M <sub>3</sub> C <sub>2</sub>	mat.FCC + M <sub>7</sub> C <sub>3</sub> + M <sub>3</sub> C <sub>2</sub>	mat.FCC + M <sub>7</sub> C <sub>3</sub> + M <sub>3</sub> C <sub>2</sub>
Ni35	mat.FCC + M <sub>3</sub> C <sub>2</sub>	mat.FCC + M <sub>3</sub> C <sub>2</sub>	mat.FCC + M <sub>3</sub> C <sub>2</sub>
Ni40	mat.FCC + M <sub>3</sub> C <sub>2</sub> + graphite	mat.FCC + M <sub>3</sub> C <sub>2</sub> + graphite	mat.FCC + M <sub>3</sub> C <sub>2</sub> + graphite
Ni45	mat.FCC + M <sub>3</sub> C <sub>2</sub> + graphite	mat.FCC + M <sub>3</sub> C <sub>2</sub> + graphite	mat.FCC + M <sub>3</sub> C <sub>2</sub> + graphite
Ni50	mat.FCC + M <sub>3</sub> C <sub>2</sub> + graphite	mat.FCC + M <sub>3</sub> C <sub>2</sub> + graphite	mat.FCC + M <sub>3</sub> C <sub>2</sub> + graphite

Table 2. Mass fractions and chromium contents of the matrix at the temperatures of the oxidation tests (according to Thermo-Calc)

mass.% of matrix	wt.%Cr in matrix	1000°C		1100°C		1200°C	
Ni25		76.10	12.96	75.40	13.26	74.62	13.76
Ni30		76.64	12.96	76.61	13.26	75.53	13.27
Ni35		75.15	11.27	75.67	11.78	76.23	12.33
Ni40		73.04	9.26	73.74	10.03	74.44	10.76
Ni45		72.49	9.26	73.19	10.03	73.88	10.76
Ni50		71.93	9.26	72.63	10.03	73.31	10.76

Table 3. Average depths of the carbide-free zone

Carbide-free zone depth ( $\mu\text{m}$ )	1000°C	1100°C	1200°C
Ni25	19 $\pm$ 1	30 $\pm$ 2	64.9 $\pm$ 8
Ni30	11 $\pm$ 1	15 $\pm$ 2	44 $\pm$ 5
Ni35	9 $\pm$ 1	18 $\pm$ 3	76 $\pm$ 12
Ni40	12 $\pm$ 2	15 $\pm$ 1	130 $\pm$ 7
Ni45	23 $\pm$ 5	34 $\pm$ 11	160 $\pm$ 3
Ni50	0 ?	50 $\pm$ 14	122 $\pm$ 4

Table 4. Minimal chromium weight contents near the external surface and average chromium content gradients across the carbide-free zone (one WDS profile per oxidized alloy)

wt.%Cr on surface	average Cr gradient in the cfz (wt.%Cr/ $\mu\text{m}$ )	1000°C		1100°C		1200°C	
Ni25		13.7	0.005	14.4	0.018	17.3	0.029
Ni30		13.5	0.106	13.5	0.010	17.5	0.018
Ni35		10.4	0.032	11.1	0.059	17.3	0.021
Ni40		9.0	0.028	10.4	0.023	16.0	0.019
Ni45		9.3	0.001	11.0	0.018	15.4	0.029
Ni50		10.1	/	10.6	0.012	14.4	0.074

Table 5. Estimated values of the masses of chromium lost per cm<sup>2</sup> of external surface by the alloys during oxidation (difference between 30wt.% and the average new Cr content in the carbide-free zone)

Loss of Cr in the carbide-free zone (mg/cm <sup>2</sup> )	1000°C	1100°C	1200°C
Ni25	2.33-2.60	3.50-3.93	5.10-6.93
Ni30	1.18-1.41	1.82-2.15	3.91-4.78
Ni35	1.32-1.64	2.31-3.11	6.20-8.59
Ni40	1.78-2.37	2.22-2.54	13.0-14.5
Ni45	3.04-4.69	3.57-6.87	16.9-17.4
Ni50	/	5.75-9.87	12.8-13.7

Table 6. Estimated values of the masses of carbon lost per cm<sup>2</sup> of external surface by the alloys during oxidation (assuming that carbon is negligible in the carbide-free zone by comparison with the initial carbon content)

Loss of C in the carbide-free zone (mg/cm <sup>2</sup> )	1000°C	1100°C	1200°C
Ni25	0.36-0.40	0.57-0.64	1.15-1.48
Ni30	0.25-0.30	0.33-0.39	0.98-1.19
Ni35	0.24-0.29	0.44-0.59	1.81-2.51
Ni40	0.34-0.46	0.46-0.53	3.99-4.44
Ni45	0.66-1.02	0.85-1.63	5.74-5.92
Ni50	/	1.50-2.58	4.77-5.10

FIGURES

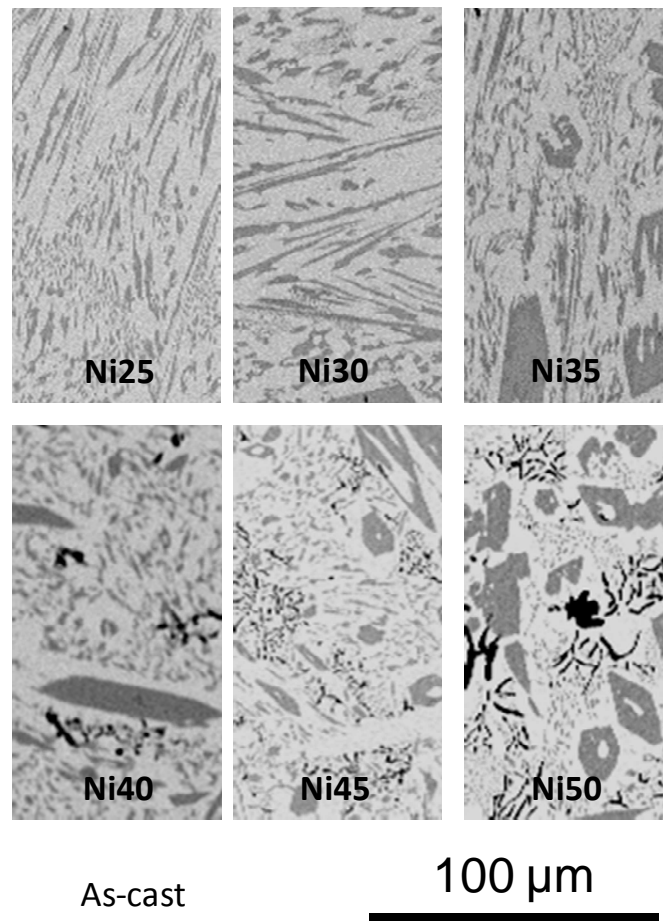


**Figure 1.** The as-cast microstructures of the studied nickel-base alloys

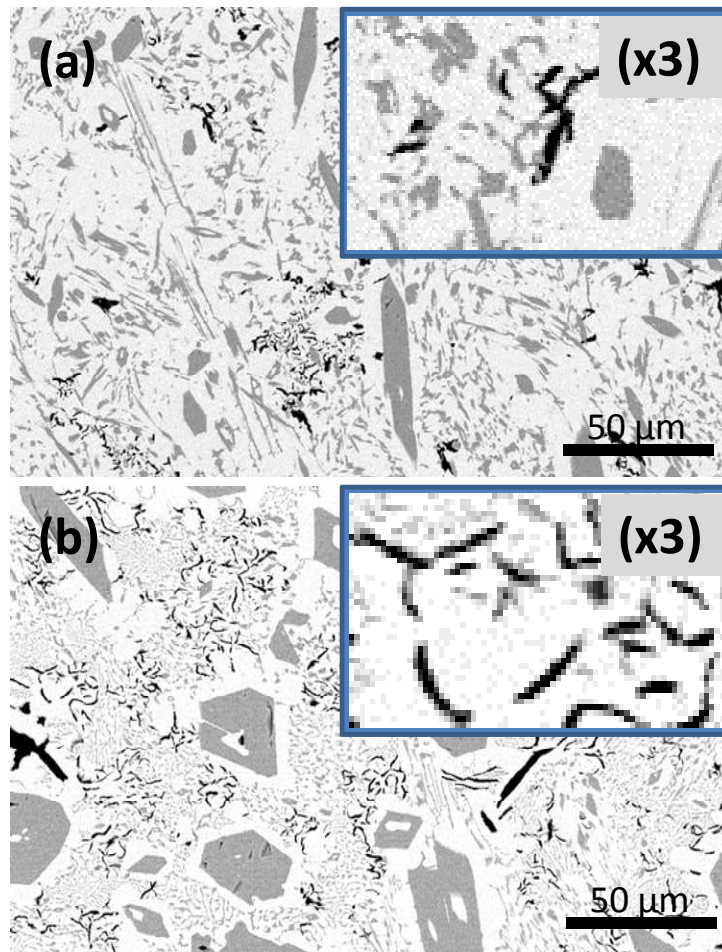


**Figure 2.** Shapes and repartitions of graphite in the Ni40 (a) and Ni50 (b) as-cast alloys graphite rare and compact in Ni40 and more present and elongated in Ni50

(“x3” means that the magnification in the two smallest micrographs are three times higher than the other micrographs’ ones)

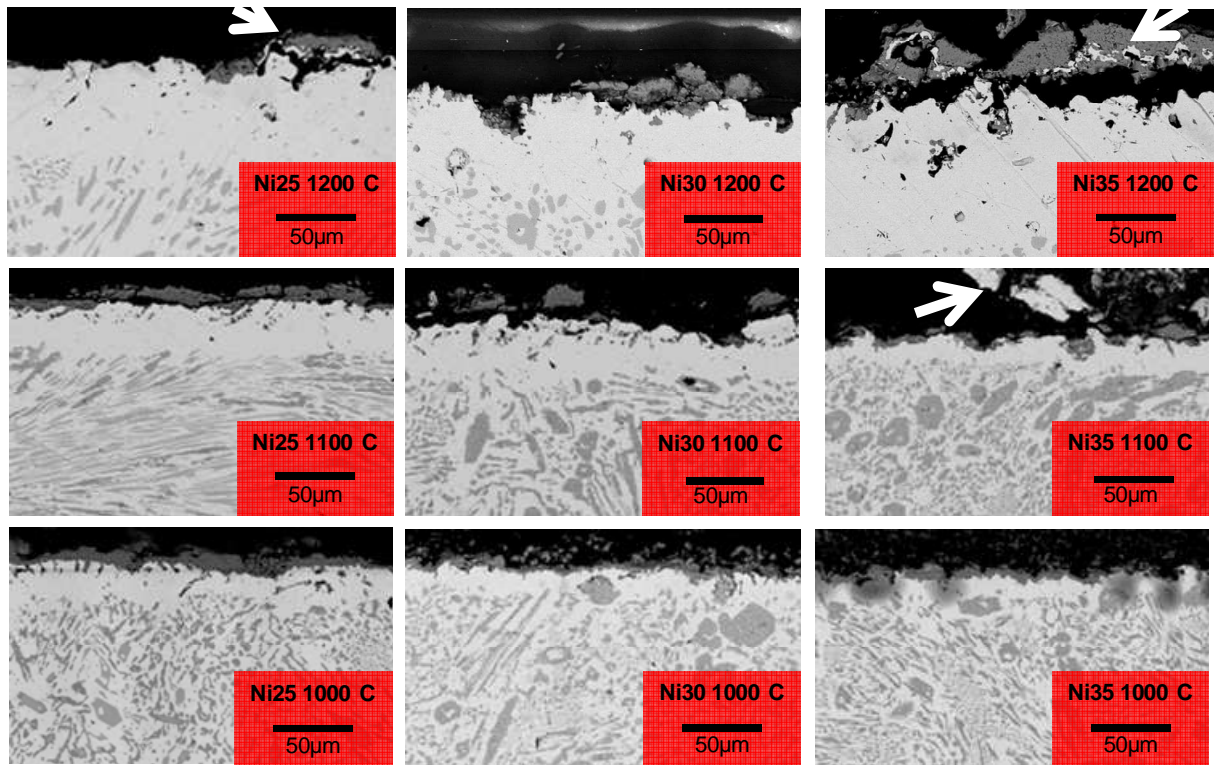


**Figure 3.** External oxides scales and sub-surface states of the alloys Ni25, Ni30 and Ni35 after 50h of oxidation in air at 1000, 1100 and 1200°C

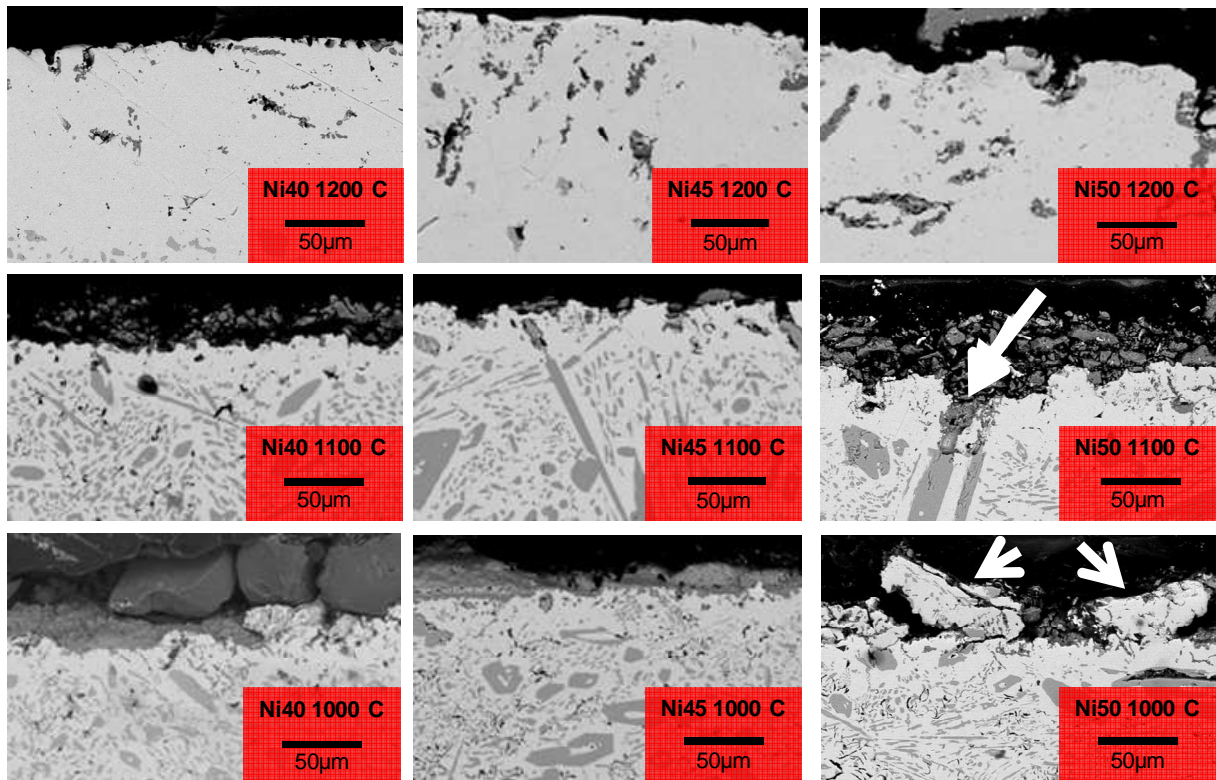


**Figure 4.** External oxides scales and sub-surface states of the alloys Ni40, Ni45 and Ni50 after 50h of oxidation in air at 1000, 1100 and 1200°C

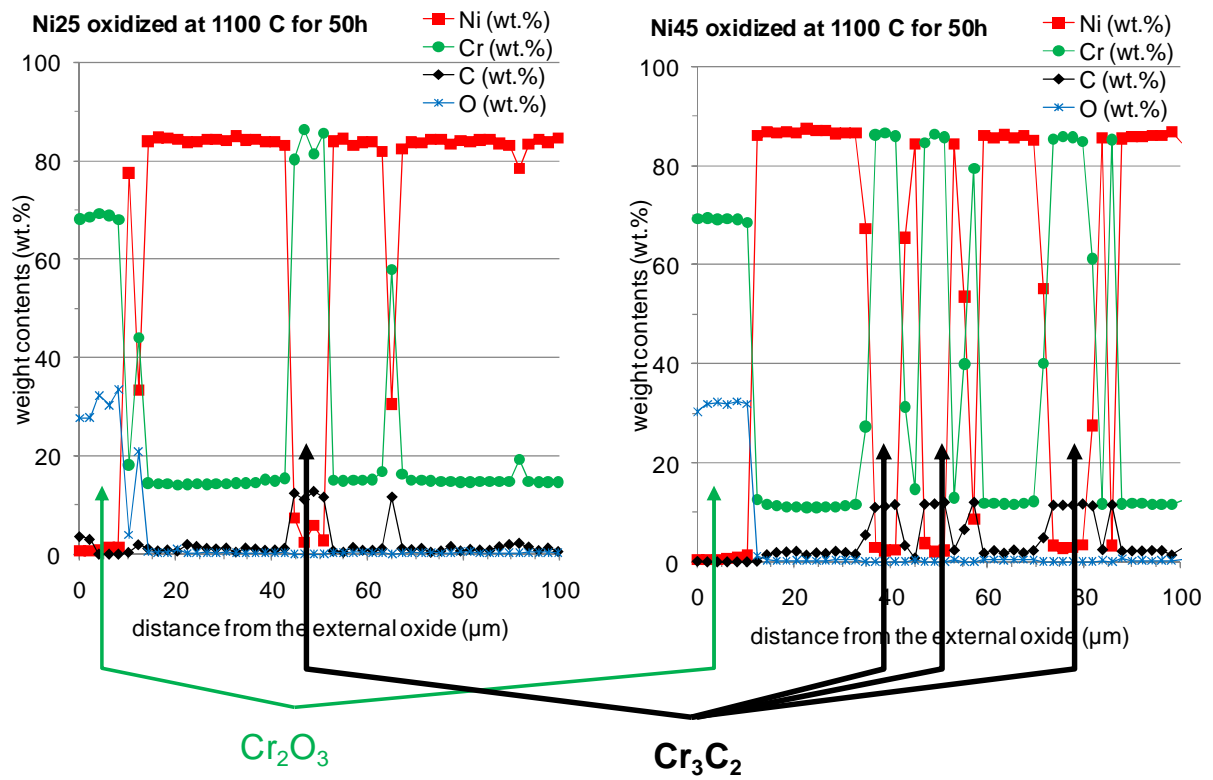


**Figure 5.** Concentrations' profiles across the external oxide scale and the sub-surface (example of Ni25 and Ni45 oxidized for 50h at 1100°C)

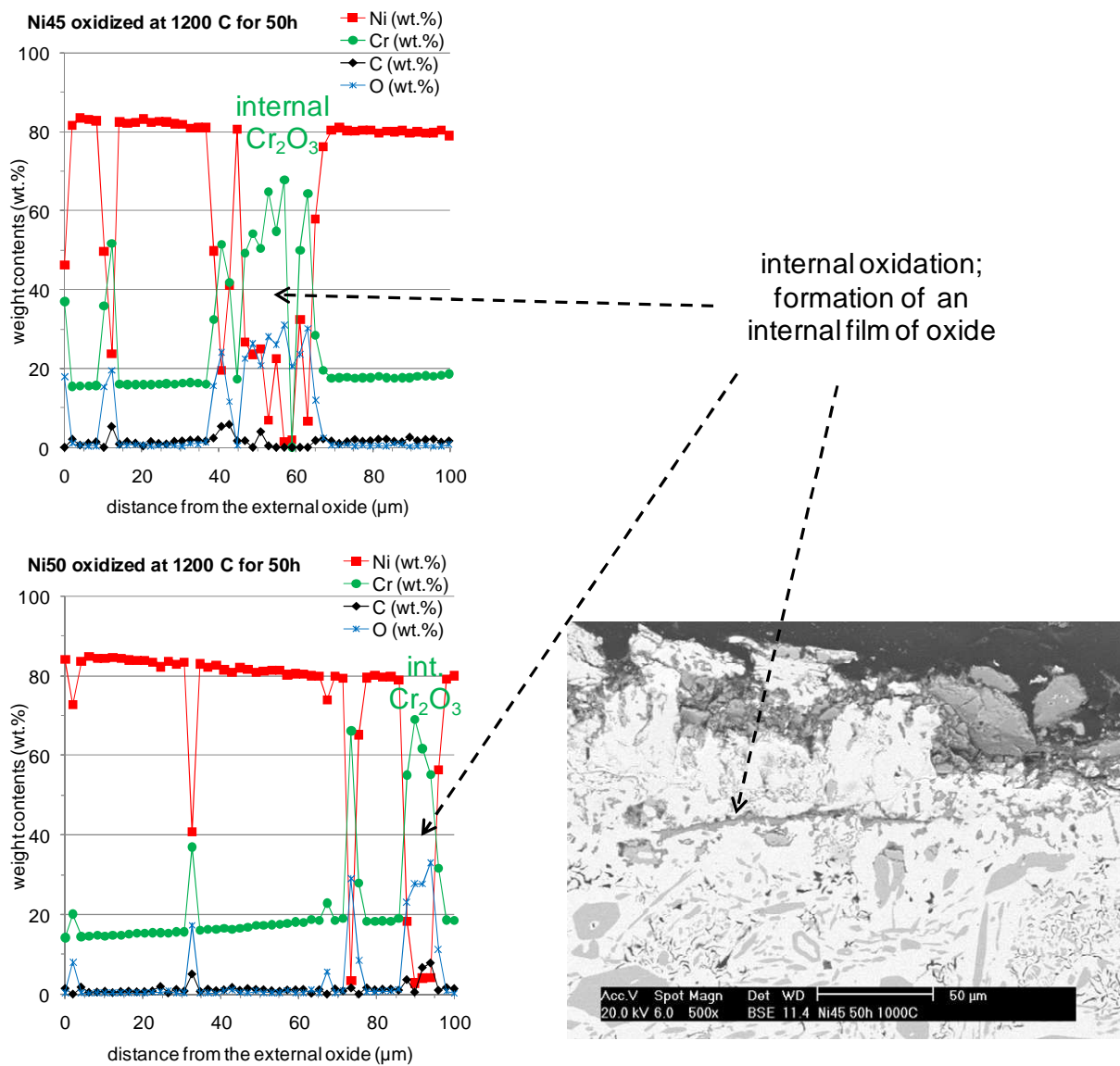


**Figure 6.** Internal chromia oxide evidenced in the sub-surface; shape resulting from the oxidation of a coarse carbide almost parallel to surface and favoring alloy spallation

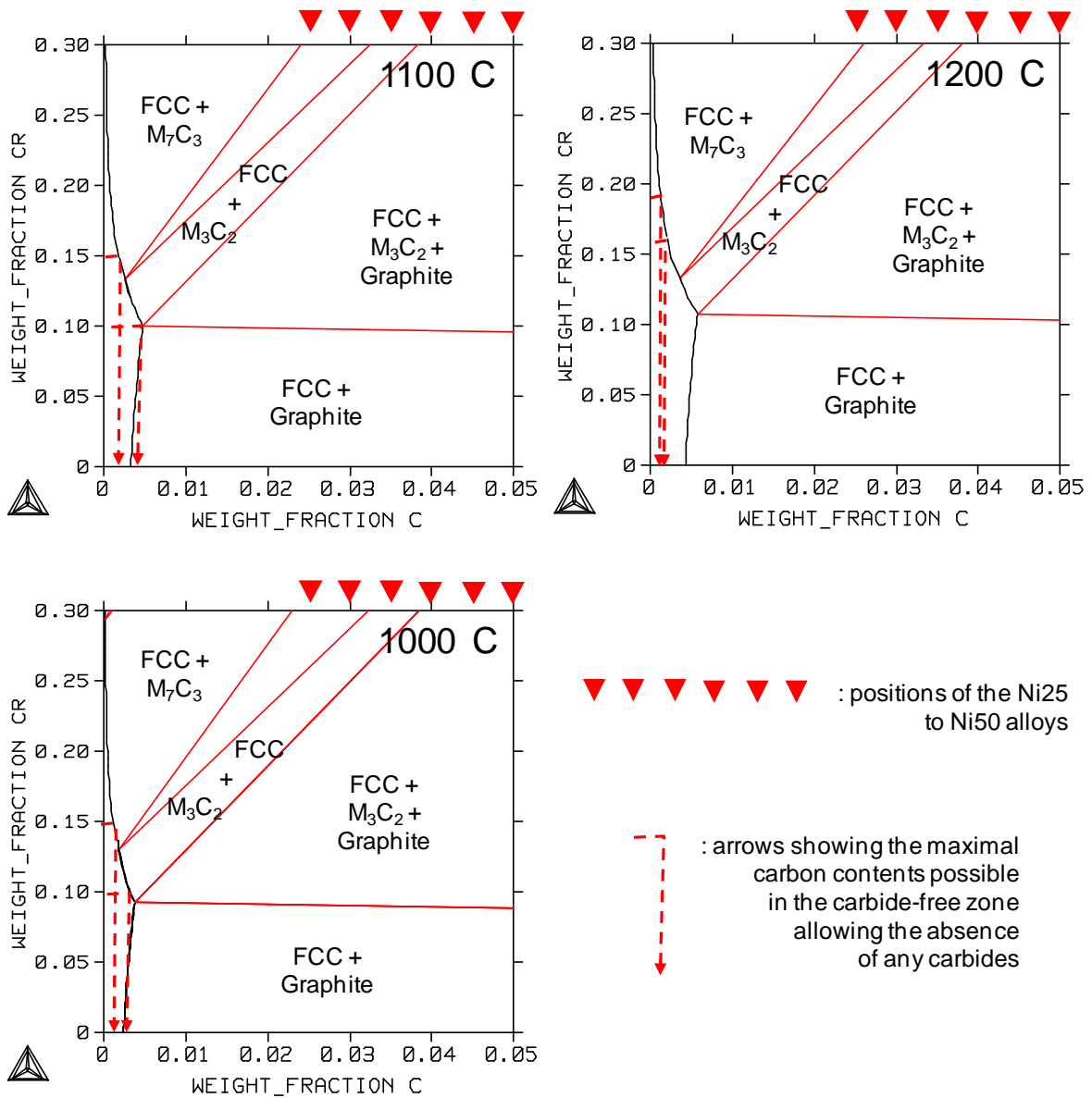


**Figure 7.** Isothermal sections of the Ni-Cr-C diagram computed with Thermo-Calc for determining the maximal local carbon contents compatible with the average chromium content and the absence of carbides in the carbide-free zones

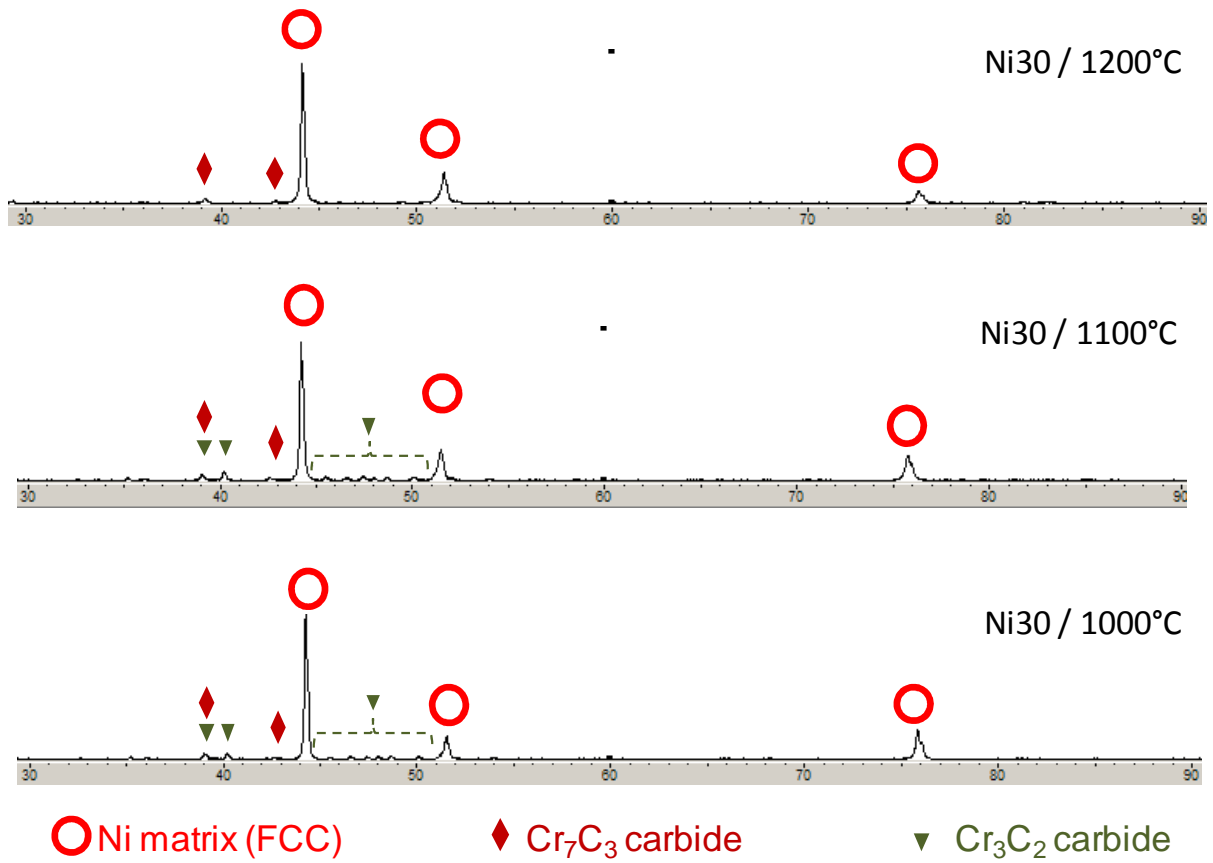


**Figure 8.** X-Ray Diffraction spectra showing the natures of the carbides in the bulk of one of the C-lowest alloys of the study (Ni30) after exposure to 1000°C, 1100°C and 1200°C

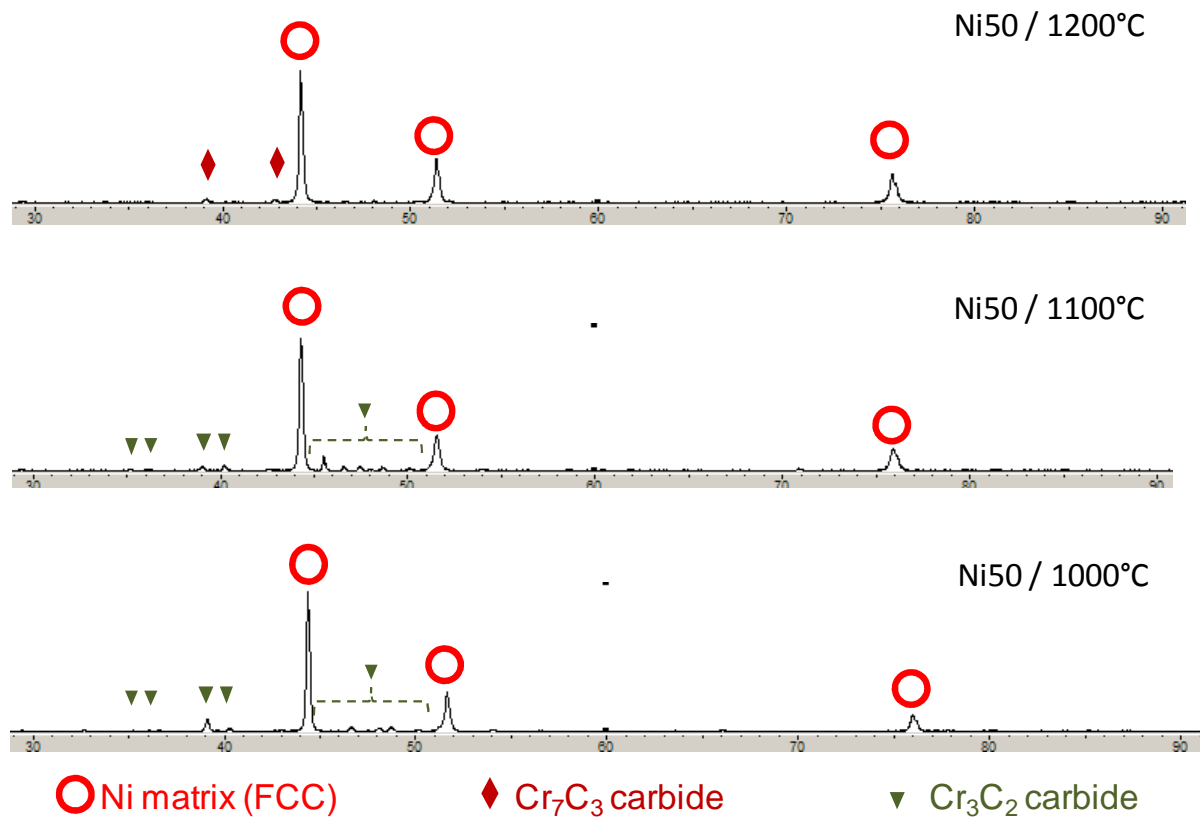


**Figure 9.** X-Ray Diffraction spectra showing the natures of the carbides in the bulk of one of the C-richest alloys of the study (Ni50) after exposure to 1000°C, 1100°C and 1200°C

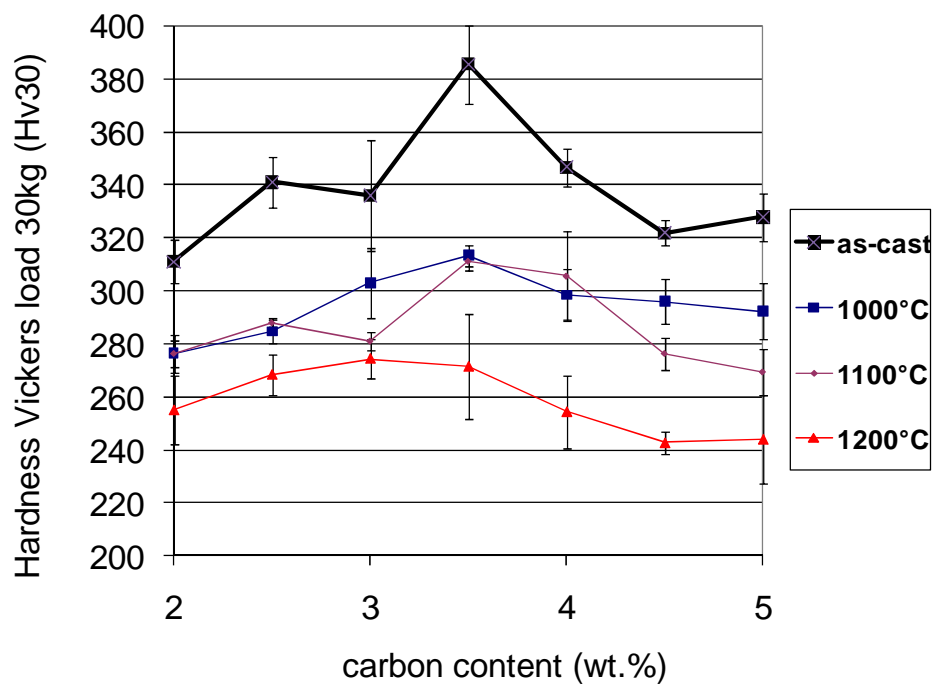


**Figure 10.** Vickers hardness of the bulk of the as-cast alloys and of the oxidized samples

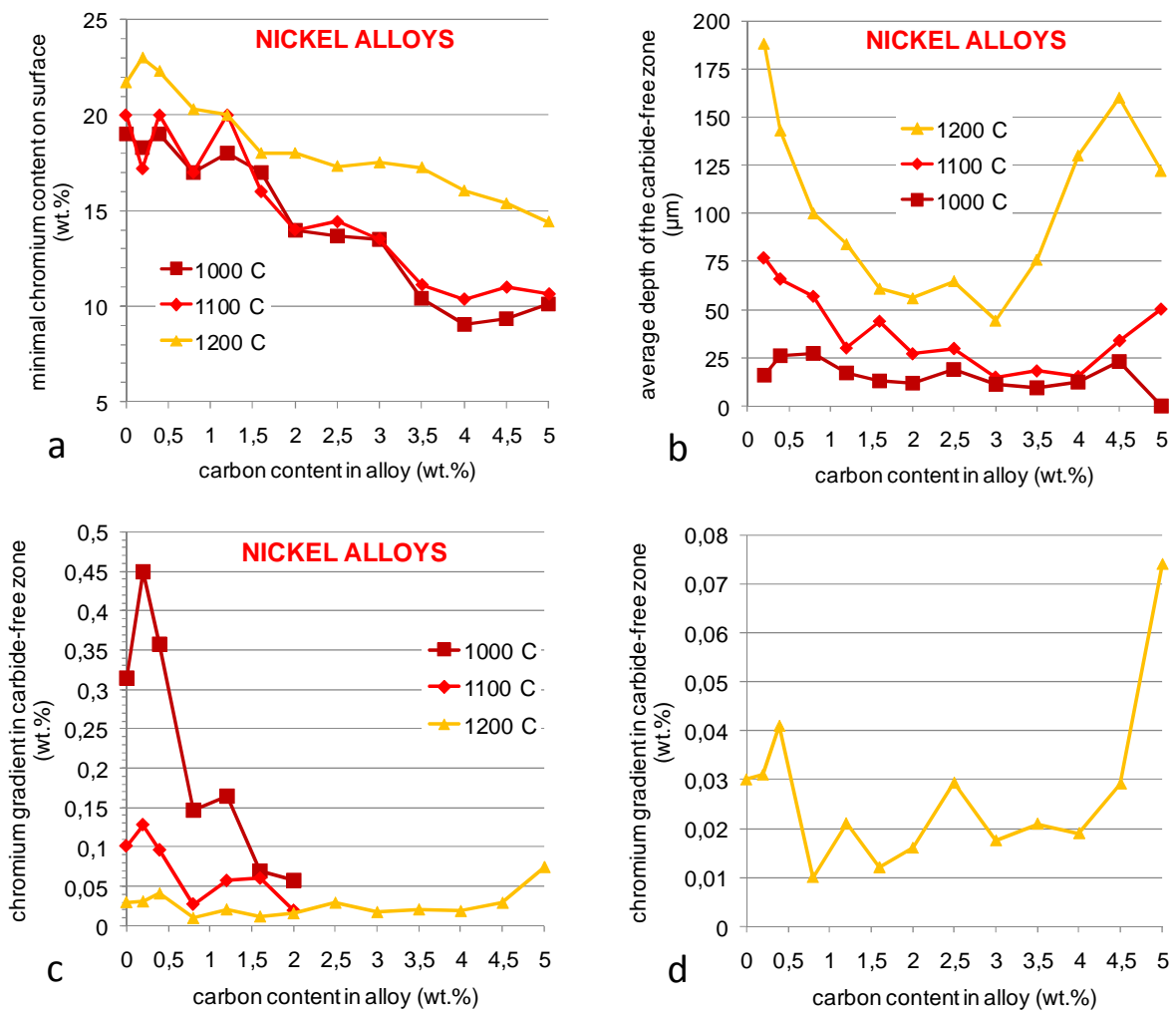


**Figure 11.** The minimal chromium content (a), the average carbide-free zone depth (b) and the average chromium gradient in the carbide-free zone (c) enlarged in (d), plotted versus the carbon content for the Ni-30Cr-0 to 2wt.%C alloys earlier studied [22, 23] and the Ni-30Cr-2.5 to 5wt.%C alloys of the present work